A Stereological Method for the Quantitative Evaluation of Cartilage Repair Tissue

Cartilage
2015, Vol. 6(2) 123–132

DOI: 10.1177/1947603514560655
cart.sagepub.com
SAGE

A Stereological Method for the Quantitative Evaluation of Cartilage Repair Tissue

Casper Bindzus Foldager[1,2,3], Jens Randel Nyengaard[4], Martin Lind[5], and Myron Spector[1,2]

Abstract

Objective: To implement stereological principles to develop an easy applicable algorithm for unbiased and quantitative evaluation of cartilage repair. *Design*: Design-unbiased sampling was performed by systematically sectioning the defect perpendicular to the joint surface in parallel planes providing 7 to 10 hematoxylin–eosin stained histological sections. Counting windows were systematically selected and converted into image files (40-50 per defect). The quantification was performed by two-step point counting: (1) calculation of defect volume and (2) quantitative analysis of tissue composition. Step 2 was performed by assigning each point to one of the following categories based on validated and easy distinguishable morphological characteristics: (1) hyaline cartilage (rounded cells in lacunae in hyaline matrix), (2) fibrocartilage (rounded cells in lacunae in fibrous matrix), (3) fibrous tissue (elongated cells in fibrous tissue), (4) bone, (5) scaffold material, and (6) others. The ability to discriminate between the tissue types was determined using conventional or polarized light microscopy, and the interobserver variability was evaluated. *Results*: We describe the application of the stereological method. In the example, we assessed the defect repair tissue volume to be 4.4 mm^3 (CE = 0.01). The tissue fractions were subsequently evaluated. Polarized light illumination of the slides improved discrimination between hyaline cartilage and fibrocartilage and increased the interobserver agreement compared with conventional transmitted light. *Conclusion*: We have applied a design-unbiased method for quantitative evaluation of cartilage repair, and we propose this algorithm as a natural supplement to existing descriptive semiquantitative scoring systems. We also propose that polarized light is effective for discrimination between hyaline cartilage and fibrocartilage.

Keywords

cartilage repair, stereology, histomorphometry, histology

Introduction

Management of focal cartilage lesions has compelled a variety of surgical repair methods such as microfracture and autologous chondrocyte implantation, and novel treatment modalities are constantly introduced. These are routinely, and necessarily, evaluated in large animal models (*viz.*, dogs, sheep, and goats) prior to introduction into the clinic, bringing attention to the methodology employed for the evaluation of the results, including the amount and types of tissue filling the defects: hyaline cartilage, fibrocartilage, and fibrous tissue.

Several histological scoring systems are available for semiquantitative evaluation of cartilage regeneration and repair *in vitro*[1,2] and *in vivo*,[3-9] and an algorithm for selecting the most suitable evaluation score has been proposed.[10] The scoring systems consist of a number of subcategories, and the score of each category is then pooled into a total score. This gives rise to potential confounding in the interpretation of the outcome as two histologically very different repair tissues might have equal scores. No single subcategory in any of these scores has been identified as having a superior predictive value as a prognostic factor. In addition, semiquantitative scores are generally believed to have poor comparability and reproducibility compared with quantitative methods.[11,12]

Supplementary material for this article is available on the *Cartilage* website at http://cart.sagepub.com/supplemental.

[1]Orthopaedic Research, Brigham & Women's Hospital, Harvard Medical School, Boston, MA, USA
[2]Tissue Engineering, VA Boston Healthcare System, Boston, MA, USA
[3]Orthopaedic Research Lab, Institute for Clinical Medicine, Aarhus University Hospital, Aarhus, Denmark
[4]Stereology and EM Laboratory, Centre for Stochastic Geometry and Advanced Bioimaging, Aarhus University, Aarhus, Denmark
[5]Sports Trauma Clinic, Aarhus University Hospital, Aarhus, Denmark

Corresponding Author:
Casper Bindzus Foldager, Orthopaedic Research Lab, Aarhus University Hospital, Nørrebrogade 44, Building 1A, 8000 Aarhus C, Denmark.
Email: foldager@clin.au.dk

Quantitative methods have also been employed for the evaluation of the amounts of various tissue types in cartilage defects in large animal models, based on counting the number of grid openings, 60 μm × 60 μm, in the eyepiece of a microscope containing a specific tissue type[13] and by tracing the area of the tissue on a digitized micrograph.[14] Whereas these methods generate data amenable to parametric statistical evaluation, they do not strictly adhere to stereological technique. For these reasons, an unbiased, reproducible, quick, and purely quantitative evaluation of the repair tissue, based on stereological principles, is a much-needed supplement to the existing methods.

Stereological methods use two-dimensional (2D) data to provide information about volume, surface area, length, and number of structural components in three-dimensional (3D) structures. The accuracy of the method and the avoidance of bias depend on a set of prerequisites and principles that must be followed.[15,16] Histomorphometric analyses using stereological principles generally consist of two steps, to which sets of rules apply: (1) the sampling of the tissue and (2) the method for quantitative estimation. Following tissue sampling, a grid consisting of the selected probes is superimposed onto the sections. Counting of the positive events (e.g., points hitting a structure or line intersections) can then be performed, and the data are analyzed using appropriate methods. Similar to other statistical principles, it is important to note that design-unbiased stereological principles are not verified or validated by experimental data but rather by mathematical proofs.[16] The precision of unbiased methods will increase with repetition, whereas assumption-based (biased) methods will tend to become more inaccurate with repetition, because of a systematic deviation from the true value. Hence, an accurate and simple algorithm is required for correct and unbiased histomorphometric evaluation of cartilage repair tissue.

The aim was to implement stereology into an easy and quickly applied algorithm for the quantitative evaluation of the volumes of various tissue types comprising cartilage repair. We hypothesized that cartilage repair tissue can be quantitatively evaluated using a design-based stereological method based on the Cavalieri estimator[15] and by assigning tissue types into well-defined histomorphology-based categories. The stereological method based on the Cavalieri estimator states that the volume of any object can be estimated if the position of the first slice hitting the object is random, that the slices are parallel, and that the thickness of the slices is known.

Methods

Reparative Cartilage Example

The goat study described in this article was approved by the Institutional Animal Care and Use Committee of the Veterans Affairs Boston Healthcare System. The stereological method is exemplified by evaluation of the reparative tissue in one cylindrical chondral defect (3 mm in diameter; depth 0.7 mm) in a caprine model, 12 weeks postoperative. Because of the thickness of caprine articular cartilage, the subchondral bone was violated and bleeding was observed. No treatment was applied. This stereological method could be applied to any relevant animal model for cartilage repair, with different treatments and follow-up times. Tissue preparation for histomorphometry followed standard laboratory protocols for chemical fixation and embedment in paraffin. Sections with a thickness of 7 μm were cut on a microtome and mounted consecutively on microscope slides and stained with hematoxylin and eosin (H&E). Other tissue processing, embedding, and sectioning protocols may be used as well.

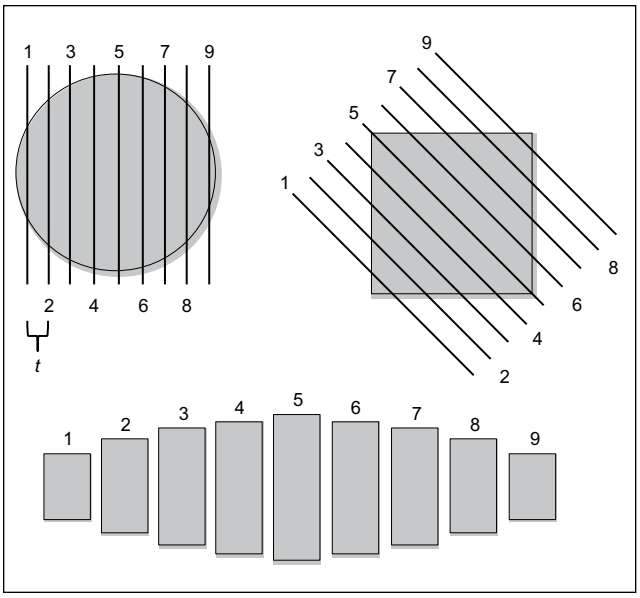

Figure 1. Sampling of a circular defect (top left) and a rectangular defect (top left) with a constant spacing, *t*, and the nine resulting sections (bottom). Sampling of irregular shapes can be performed similarly resulting in a number of sections with different sizes. The location of the first section (1 on the figure) is chosen randomly to avoid bias. To ensure that the evaluated feature is represented in varying sizes on the sections, sectioning of rectangular defects must be performed as depicted in the figure.

Sampling Strategy

In order to limit the risk of bias, the location of the first histological section to be analyzed should be selected at a random start position. The goal is to analyze 7 to 10 sections through the defect site with (1) a known spacing between respective sections and (2) the evaluated feature (e.g., repair tissue) represented in varying sizes.[15] The most effective sampling method is depicted in **Figure 1**. Using

this method, sections distributed throughout the whole defect are obtained. Note that the described method is not suitable for detection of "rare events," that is, features comprising less than 2% of the total region of interest. The researcher determines the region of interest but will in most cases be the original defect area (chondral or osteochondral) depending on the outcomes needed in the selected cartilage repair model. The distance between the sections, *t*, is determined by dividing the length of the sampling area (e.g., the diameter of the circle in **Fig. 1**) by the number of sections needed. For this cartilage repair example, the sections are cut perpendicular to the surface of the joint to ensure that the size of evaluated volume on the cross sections is not overestimated.

Preparation of Images for the Point Counting Process

The goal of preparing images for the point counting process is to obtain a number of viewing windows (sections on which something is counted; "counting-images") in a random and systematic manner. To ensure random sampling and to limit the risk of bias, the first window is randomly selected. A constant spacing between the viewing windows will ensure a systematic sampling. A total number of 40 to 50 viewing windows are required per defect to provide an estimate with high precision.[16] Grid spacing is adjusted so that the test point on the 7 to 9 sections with approximately 40 to 50 viewing windows will provide 100 to 200 positive counts. The magnification must be the lowest possible that allows for safe discrimination between positive and nonpositive hits. In our example, magnification 10× was used. Spacing between viewing windows was 0.8 mm in the horizontal axis and 0.4 mm in the vertical axis. In each viewing window, there were 9 points for counting in the total volume estimation and 25 points for counting in the tissue composition evaluation. Spacing and number of points per viewing window could be adjusted according to the size of the section. Pilots may have to be performed to ensure that approximately 200 positive hits are counted for each estimate.

Commercial stereological systems that provide automated and systematic movement of the microscopic slide in a predetermined fashion are reliable, very fast, and easy to use. These systems are, however, expensive. There are two inexpensive alternative methods for obtaining the same results.

1. If the defect area on the slides is big (i.e., the number of necessary viewing windows will have a spacing of at least ¼ mm), the ruler in the microscope can be used with reliable results.
2. For smaller defects, images of the whole defect (with overlap) are obtained with the magnification needed for the subsequent evaluation.

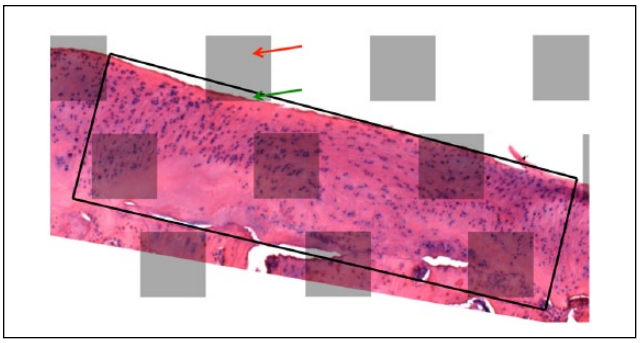

Figure 2. The region of interest (original defect area) is delineated (black lines) and viewing windows are distributed on the image. The images should be slightly rotated to avoid bias in such layered tissues. Note that in the selection of images for analysis it is important to avoid risk of over- and underrepresentation of specific topographical zones. To calculate an estimate of defect fill points hitting within the region of interest but not hitting tissue (green arrow) must be counted in a category named, for example, "empty." Points hitting outside the region of interest (red arrow) should not be counted.

These images can easily be merged using inexpensive software such as online image mergers or alternatively Adobe Photomerge tool. On the merged image the viewing windows can be systematically selected and saved as separate image files in jpeg format (**Fig. 2**). The high magnification ensures that they can be used for evaluation.

Point Counting

It is a prerequisite of the counting method that the sum of the dimensions (D) of the region be analyzed, and the dimensions of the "probe" should equal at least three. Thus, estimation of volumes (3 D) can be performed by point counting (i.e., a probe of zero dimensions, 0 D). Point counting can be performed using commercial software packages such as newCAST (Visiopharm, Hørsholm, Denmark). In addition, we suggest the use of a newly developed and free online software, the STEPanizer.[17] The manual and a practical guide can be found at www.stepanizer.com.

Briefly, the first image file is selected and the number of counting points per viewing window is set. Each point hitting a structure is counted using the numerical pad on the keyboard. For evaluation of cartilage repair defects the counting is performed in two steps: (1) in the first step, low magnification is used for the estimation of the repair tissue volume and potentially for the calculation of tissue filling; and (2) in the second, a higher magnification is employed to allow for evaluation of the various tissue types. When estimating the volume of the repair tissue, the points hitting any tissue within the repair area or defect is counted as positive. If the original articulating surface can be estimated and

Table 1. Tissue Categories.

Tissue Type	Definition
Hyaline cartilage	Rounded cells in lacunae in cartilage matrix
Fibrocartilage	Rounded cells in lacunae in fibrous matrix
Fibrous tissue	Elongated cells in fibrous matrix
Bone	Woven or lamellar bone
Scaffold material	Remnants of implanted material
Others	Blood vessels, bone marrow, etc.

outlined, the points hitting within the original defect area but not hitting tissue can be assigned to a new category "empty" (**Fig. 2**). This will allow for the estimation of the amount of tissue filling the defect with a very high precision. Another method for calculating defect fill can be performed by using the estimated repair tissue volume by counting points hitting tissue within the defect area and dividing this by the original defect volume when this is known. For evaluation of the amount of the different tissue types, we selected the tissue types that can be present in a cartilage defect. These were assigned into categories as shown in **Table 1**. To improve the efficiency of the counting, we added simple, validated, and easily distinguishable definitions of the different tissue types. Examples of these tissues can be found in the supplemental data.

When a point lands on (i.e., "hits") a specific tissue within the selected repair or defect area, the point is counted within the category (**Table 1**) corresponding to the tissue type (**Fig. 3**). Points hitting outside the defect area are left uncounted unless needed for calculation of tissue filling. Following point counting in each viewing window (image), the data are saved in a Microsoft Excel spreadsheet in which relevant calculations can be made or the data can be retrieved and used in other programs. If the total number of positive counts is denoted, P, the area per point is (a/p), and if the distance between the slides is t, then the volume, V, is calculated as follows:

$$V = \sum P \cdot \frac{a}{p} \cdot t$$

The tissue fractions are calculated by dividing the positive counts for a tissue by the total counts hitting any tissue type within the defect.

Precision of the Method

Calculation of the precision of the estimation of the percentage of specific tissue types in the defect involves two factors: (1) the observer's ability to distinguish the tissue types based on prescribed definitions (**Table 1**) and (2) the precision of the stereological method.

To determine the ability of independent observers to recognize the specified tissue types, specific sections were chosen with a fixed set of counting points. The distinction between hyaline cartilage and fibrocartilage was based on the classical histological difference in the fibrous appearance of the matrix. The matrix of hyaline cartilage appears "glass-like" whereas the chondrocytes in fibrocartilage are dispersed among collagen fibers[18] Reliance on immunohistochemical staining of type I collagen (fibrocartilage) and type II collagen (hyaline cartilage) for this distinction is limited because (1) fibrocartilage can contain type II collagen,[18] (2) there are risks of false negatives and false positives with the immunohistochemical technique, and (3) adequate experience with the technique is not widely available. Polarized light microscopy images were used to differentiate between hyaline cartilage and fibrous cartilage based on the birefringent appearance of distinct collagen fibers, particularly in sections in which the distinction was questionable using conventional transmitted light alone (**Fig. 4**). The orientation of the collagen relative to the articular surface, by polarized light microscopy, in order to determine if the hyaline cartilage had the feature (i.e., the arcuate orientation of collagen) of articular cartilage was not investigated. Six independent observers were then asked to assign each point on the H&E sections to a tissue category. All images were produced in both conventional and polarized light.

The error variance of the Cavalieri estimator is based on a mathematical model from Gundersen and Jensen.[15] The risk of bias relies on the ability to follow the method for systematic sampling as described above. The total variance of the estimate of the total volume is the sum of the statistical *noise effect* of the estimate (P_i) and the *variance* of the area (a). For calculations of the precision of the estimate, it is useful to make a table in which necessary values are calculated (**Table 2**). The *noise* and *variance* can then be calculated as follows:

$$Noise\ (P_i) = 0.0724 \cdot \left(\frac{b}{\sqrt{a}}\right) \cdot \sqrt{n \cdot \sum P_i}$$

$$Var\left(\sum a\right) = \frac{\left(3 \cdot \left(\sum \left(P_i \cdot P_i\right) - Noise\right) - 4 \cdot \left(\sum \left(P_i \cdot P_{i+1}\right) - \sum \left(P_i \cdot P_{i+2}\right)\right)\right)}{\sum P_i}$$

$$Var\left(Total\right) = Noise + Var\left(\sum a\right)$$

$\left(\frac{b}{\sqrt{a}}\right)$ is the average profile shape, which can be estimated from the normogram found in previous work by Gundersen and Jensen.15 The precision, or coefficient of error (CE), is then calculated as follows:

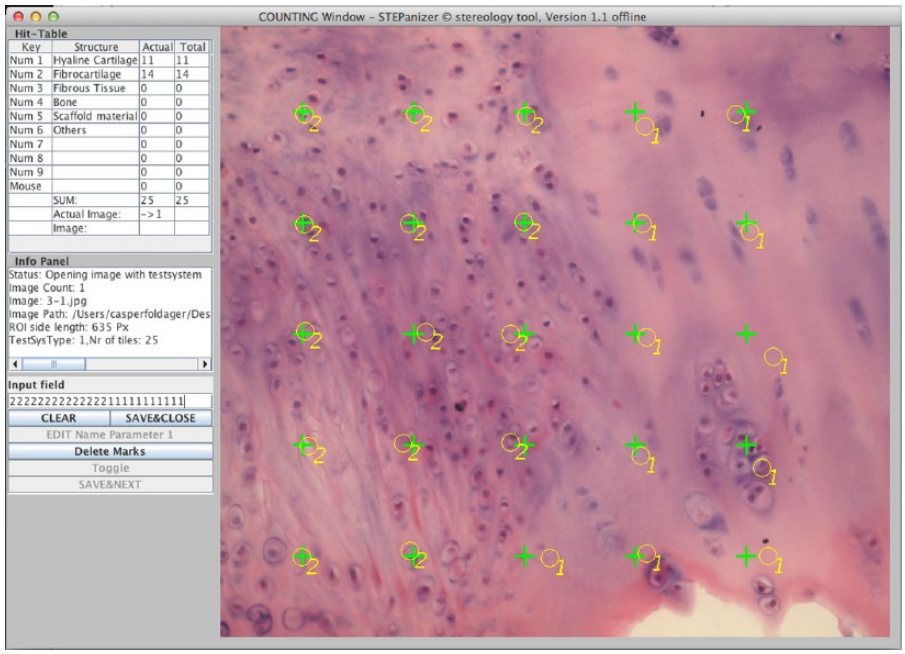

Figure 3. The STEPanizer counting window. H&E-stained section with superimposed counting probes (green points) and the actual counted points (numbered yellow circles). The yellow counted points does not need to hit the actual counting probes as it is the number of hits and not their location that is saved. Hence, these yellow points are only used to manage which points have been counted. Note that it is the single point depicted by the arrow that represents point/pixel that is counted and not the whole cross or center of the cross itself.

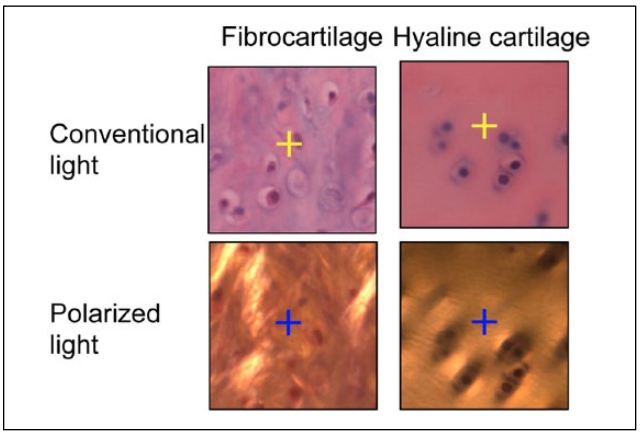

Figure 4. Morphologic appearance in conventional and polarized light microscopy of fibrocartilage and hyaline cartilage. Cell reside in lacunae in both tissues differences are visible in the appearance of the extracellular matrix.

$$CE\left(\sum P\right) = \frac{\sqrt{Var\left(Total\right)}}{\sum P}$$

Tissue Discrimination and Interobserver Variability

Six blinded investigators (PhD student to professor level including two cartilage repair surgeons) with experience in cartilage repair were sent a simple instruction sheet (see Supplemental materials) along with seven different H&E-stained histological images with counting points of the tissue types appearing in cartilage repair. Based on the information given in the instruction sheet they evaluated the amount of different cartilage repair tissues on seven histological images in H&E (Test 1). Two weeks after completion of the evaluation of the H&E-stained histological sections, an additional test was sent to the observers with similar images stained with H&E, but obtained under polarized light (Test 2; **Fig. 5**). The ability to recognize specific tissue types in images obtained under either normal or polarized light was calculated and presented as mean ± SD.

Results

The algorithm was used to evaluate cartilage from a square cylindrical defect as described under Materials and Methods. In some situations it may be worthwhile to present the tissue fractions in percentages of the total volume, but this does not take into account the defect filling. If the aim is for a treatment to facilitate hyaline cartilage, it is more advisable to present the total volume of this tissue or the percentage of the tissue as a fraction of the total defect size.

Tissue Recognition and Interobserver Variability

Distinguishing between hyaline cartilage and fibrocartilaginous tissue proved difficult in images with only one tissue

Table 2. Example of a Table for Calculation of the Precision of the Estimate.

Section (i)	P_i	$P_i \cdot P_i$	$P_i \cdot P_{i+1}$	$P_i \cdot P_{i+2}$
1	A	$A \cdot A$	$A \cdot B$	$A \cdot C$
2	B	$B \cdot B$	$B \cdot C$	$B \cdot D$
3	C	$C \cdot C$	$C \cdot D$	$C \cdot E$
4	D	$D \cdot D$	$D \cdot E$	—
n	E	$E \cdot E$	—	—
Sum	$\sum P_i$	$\sum(P_i \cdot P_i)$	$\sum(P_i \cdot P_{i+1})$	$\sum(P_i \cdot P_{i+2})$

type present (hyaline cartilage or fibrocartilage) when the evaluation was performed under normal light. Three images in the tests contained hyaline cartilage only, fibrocartilage only, or both tissue types in the same image. In contrast, evaluators were able to, with high precision, discriminate between these two tissue types when evaluated under polarized light. In these three images determination of the tissue types under normal or polarized light lead to very different outcomes (**Fig. 5**), and the use of polarized light for discrimination between these tissue types may in this algorithm as well as in the commonly used semiquantitative scores be used to significantly limit the risk of bias.

Interobserver variation was generally low as reflected in low standard deviations (SD) of the evaluated images. The observer variability test required the observers to be able to discriminate between tissue types and to be able to determine in which tissue type a cross was placed (**Fig. 3**, right), keeping in mind that only a single pixel on the cross represents the point to be counted. SD < 25% was found with the exception of the attempt to evaluate fibrocartilage in conventional light (**Fig. 5**, left). These SDs reflect only 20 points counted on each image, and stereological principles applied ensure that when more points are counted (usually 150-200 points per sample) the estimates converge toward the true value as opposed to biased and semiquantitative evaluation systems.

Discussion

A prior review[19] examined the features of the various categorical and numerical methods employed for the histological evaluation of the reparative tissues in cartilage defects in animal models. That review underscored the limitation of the many categorical methods, for which parametric statistics are precluded from use. In this article, we describe a simple and unbiased method for quantitative (numerical) evaluation of cartilage repair based on stereology,[20] a technique that has been used for decades for the quantitative evaluation of image data from a wide array of subjects. There have been no prior published studies of cartilage repair that have employed a stereological approach.

Similar to other statistical principles, design-unbiased stereological principles are not verified or validated by experimental data but rather by mathematical proofs. Whereas estimates converge toward the true value by repetition in statistical methods, the accuracy of assumption-based (biased) methods will tend to become more inaccurate on repetition, because of a systematic deviation from the true value.[16] We showed that applying this mathematically validated algorithm in cartilage repair evaluation provides information about repair tissue composition with very precise estimates.

Because of nature of the method, the parameters related to interobserver variability are limited to the identification and distinction of tissue types. By using simple and easily identifiable characteristics for categorization in both normal and polarized light microscopy, we limit these risks. It is important to note that the evaluators had experience in cartilage repair research and histology, but were not trained using only the instruction sheet (see Supplemental material). The results depicted in **Figure 5** show that polarized light illumination is superior to conventional light microscopy when discriminating between hyaline cartilage and fibrocartilage. The ability to identify specific tissue types will improve by training, as a learning curve is expected, and the precision of the estimate would thereby increase by training. Efficiency is a fundamental aspect of stereology.[21] This favors point-counting over other approaches such as delineation of tissue compartments in which an indefinite number of choices have to be made by the evaluator drawing the line, which for all practical matters consists of thousands of points and subsequently thousands of decisions to be made by the observer.

The assessment of the precision of the stereological method in cartilage repair is principally based on the metric CE, the coefficient of error, defined as the standard deviation divided by the mean. In effect, CE is a measure of how good the estimate of a parameter by the stereological procedure is. The lower the CE the higher the confidence one can have on the precision of the method as applied to the problem at hand. In the case of estimating the tissue filling the CE was very low, 0.01. Hence, in the provided example the true tissue volume (v) estimated to be 4.35 mm^3 ($\bar{v}$) has a 95% probability of being within the range of 4.26 to 4.44 mm^3 (*i.e.,* $\bar{v} \pm 2 \times CE \times \bar{v}$) (see **Table 3**). As for any other method, the precision of the mean estimate in a group of animals will depend on the biological variability, sample size, and so on. Following the prerequisites in the unbiased sampling evaluations does not require calculation of CE values for the precision of the estimate, but it may be helpful to do so when applying the method for the first time. CE values for the tissue fractions will by nature be higher than CE for the total tissue volume. The calculation of these CE values can be estimated, but this requires highly complex mathematical calculations, which are outside the scope of

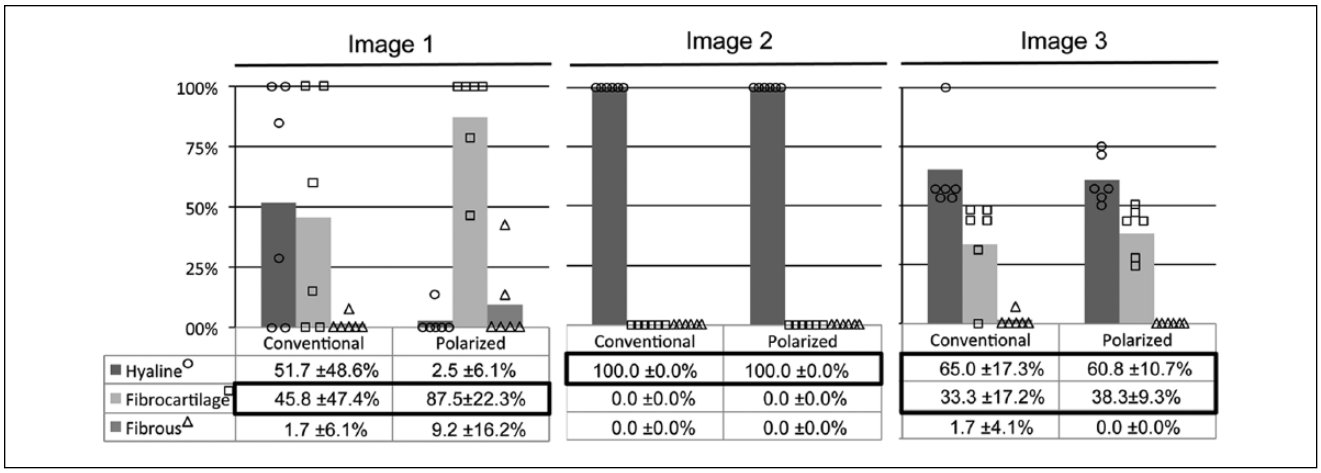

Figure 5. Mean tissue composition (±SD) on three different images (bars) from the same defect based on the point-counting evaluations from six independent and experienced observers. The three different images contained fibrocartilage only (left), hyaline cartilage only (middle), or both hyaline cartilage and fibrocartilage (right). The histological images were evaluated first in conventional light and then polarized light (left and right bars, respectively, on each image graph). The circles, squares, and triangles represent the tissue fraction assessed by each observer on each image. This shows the risk of systematic wrong assessments by evaluating fibrocartilage in conventional light compared with polarized light, because observers tend to assign points to either all hyaline cartilage or all fibrocartilage. This is also reflected in the large SD in this graph.

Table 3. Outcome Example of the Evaluation of a Cylindrical Chondral Defect on the Femoral Condyle in a Canine Model.

Total volume	4.35 mm^3
Defect fill	88.0%
Coefficient of error, *CE*	0.01
	Fractions mm^3 (%)
1. Hyaline cartilage	1.21 (27.8)
2. Fibrocartilage	2.43 (55.5)
3. Fibrous tissue	0.60 (13.7)
4. Bone	0.05 (1.1)
5. Scaffold material	0.00 (0)
6. Others	0.06 (1.4)

this article. The CE for a specific tissue type, that is, fraction of tissue filling the defect, might be as high as 0.10, meaning that the 95% confidence intervals of the would be 10 times wider than for the total volume estimate with a CE of 0.01.

Stereological principles cover a wide range of specific methods commonly applied in other specialties such as neurology, psychiatry, nephrology, cardiology, dermatology, pulmonology, and bacteriology.[22-27] In orthopedics, histomorphometry has long been used for evaluation of bone biopsies in osteomalcia and osteoporosis and arthritis as well as gold standard in regenerative approaches.[28-32] In cartilage repair, stereology has recently been used to quantify specific aspects of the repair process such as subchondral blood vessels, collagen volume and fibril surface density, and cellular composition in chitosan implant.[33-35] In osteoporosis, histomorphometric parameters such as the bone volume/total volume fraction and trabecular thickness predicts fracture risk and outcome after implant fixation. Prognostic factors in cartilage repair encounter parameters such as defect type and location,[36,37] patient age,[37,38] and prior treatment.[39] Histomorphometric parameters as positive or negative outcome predictors in cartilage repair have yet to be determined. These might include the degree of filling of a defect with reparative tissue regardless of tissue types, tissue composition, and the heterogeneity of distribution. The proposed method for evaluating cartilage repair is dynamic in the sense that other subcategories such as chondrocyte clustering and cellularity can easily be introduced and evaluated for their outcome predictability.

Stereological approaches for cartilage evaluation are not limited to histological sections. Prior studies have applied these principles for evaluation of cartilage thickness after periacetabular osteotomy using magnetic resonance imaging.[40,41] Using this imaging modality for stereological analysis, the same set of prerequisites as described here must be applied in order to obtain an unbiased estimates.

Semiquantitative scoring systems are beneficial in providing standardized ways for qualitative histology, but their specificity and reproducibility (especially for selected subcategories) are considered rather low. A previous study showed that even trained pathologists in a side-by-side comparison were not able to detect a reduction in cell number by one third.[11] Implementation of semiquantitative scores is often limited by the evaluation of only a few sections through the defect center[42] or at selected locations,[43] indicating that these would represent the morphology of the entire defect. This omission of unbiased sampling may be a

potential source of bias despite a comprehensive evaluation of the selected sections.

The use of a quantitative evaluation alone is limited by lack of the descriptive qualitative information, which may be obtained using descriptive semiquantitative scores. Hence, these two types of modalities will intuitively supplement each other very well. Immunohistochemical analyses provide information of the distribution of target proteins, which, if sampled correctly according to the aforementioned descriptions, also candidates for histomorphometric analysis, though staining inconsistencies and other issues related to immunohistochemical complicates this method.

A limitation of this study is that the stereological method was not demonstrated in a longitudinal investigation evaluating the changes with time in the percentages of the various tissue types comprising the reparative tissue induced by a particular cartilage repair method. In this article, the stereological method was applied to the reparative tissue in an untreated cartilage defect 12 weeks postoperative. The method, however, is validated as a stereological tool, regardless of the relative amounts of the various tissue types filling the lesion, and is therefore time independent. The objective of the article was to demonstrate the application of the stereological method, and this could be done at any one time point after a cartilage repair procedure.

The current article demonstrates that a stereological procedure can be implemented as an easily applied and design-unbiased method for rapid and precise quantification of tissue types in cartilage repair in histological images. The method can be used to assess the amount of tissue filling a defect as well as fractionating tissue compositions. The former can also be applied to images from other imaging modalities, including magnetic resonance imaging. Polarized light microscopy is effective in discrimination between hyaline cartilage and fibrocartilage in evaluation of cartilage repair outcome, thus limiting potential bias in the evaluation. A truly quantitative evaluation method improves the opportunity for statistical intergroup evaluations and comparisons of outcome between laboratories. We propose that this algorithm offers a natural supplement to existing descriptive semiquantitative scoring systems for evaluation of outcome in cartilage repair.

Acknowledgments and Funding

The authors would like to thank the six blinded observers participating the evaluation. We would also like to thank Niels Trolle, Department of Biostatistics, Aarhus University, for assisting in the description of interobserver variability. The research reported here was supported, in part, by the U.S. Department of Veterans Affairs, Veterans Health Administration, Rehabilitation Research and Development Service. A postdoctoral research fellowship for CBF by an Elite Research Scholarship from the Danish Minister of Science, Technology and Innovation. Centre for Stochastic Geometry and Advanced Bioimaging is supported by Villum Foundation.

Declaration of Conflicting Interests

The author(s) declared no potential conflicts of interest with respect to the research, authorship, and/or publication of this article.

Ethical Approval

The goat study described in this article was approved by the Institutional Animal Care and Use Committee of the Veterans Affairs Boston Healthcare System.

References

1. O'Driscoll SW, Marx RG, Beaton DE, Miura Y, Gallay SH, Fitzsimmons JS. Validation of a simple histological-histochemical cartilage scoring system. Tissue Eng. 2001;7:313-20.
2. Grogan SP, Barbero A, Winkelmann V, Rieser F, Fitzsimmons JS, O'Driscoll S, *et al*. Visual histological grading system for the evaluation of in vitro-generated neocartilage. Tissue Eng. 2006;12:2141-9.
3. Roberts S, McCall IW, Darby AJ, Menage J, Evans H, Harrison PE, *et al*. Autologous chondrocyte implantation for cartilage repair: monitoring its success by magnetic resonance imaging and histology. Arthritis Res Ther. 2003;5:R60-73.
4. Knutsen G, Engebretsen L, Ludvigsen TC, Drogset JO, Grøntvedt T, Solheim E, *et al*. Autologous chondrocyte implantation compared with microfracture in the knee. A randomized trial. J Bone Joint Surg Am. 2004;86:455-64.
5. O'Driscoll SW, Salter RB. The repair of major osteochondral defects in joint surfaces by neochondrogenesis with autogenous osteoperiosteal grafts stimulated by continuous passive motion. An experimental investigation in the rabbit. Clin Orthop Relat Res. 1986;(208):131-40.
6. Pineda S, Pollack A, Stevenson S, Goldberg V, Caplan A. A semiquantitative scale for histologic grading of articular cartilage repair. Acta Anat (Basel). 1992;143:335-40.
7. Wakitani S, Goto T, Pineda SJ, Young RG, Mansour JM, Caplan AI, *et al*. Mesenchymal cell-based repair of large, full-thickness defects of articular cartilage. J Bone Joint Surg Am. 1994;76:579-92.
8. Mainil-Varlet P, Aigner T, Brittberg M, Bullough P, Hollander A, Hunziker E, *et al*. Histological assessment of cartilage repair: a report by the Histology Endpoint Committee of the International Cartilage Repair Society (ICRS). J Bone Joint Surg Am. 2003;85(Suppl 2):45-57.
9. Mainil-Varlet P, Van Damme B, Nesic D, Knutsen G, Kandel R, Roberts S. A new histology scoring system for the assessment of the quality of human cartilage repair: ICRS II. Am J Sports Med. 2010;38:880-90.
10. Rutgers M, van Pelt MJ, Dhert WJ, Creemers LB, Saris DB. Evaluation of histological scoring systems for tissue-engineered, repaired and osteoarthritic cartilage. Osteoarthritis Cartilage. 2010;18:12-23.
11. de Groot DM, Hartgring S, van de Horst L, Moerkens M, Otto M, Bos-Kuijpers MH, *et al*. 2D and 3D assessment of neuropathology in rat brain after prenatal exposure to methylazoxymethanol, a model for developmental neurotoxicty. Reprod Toxicol. 2005;20:417-32.
12. de Groot DM, Bos-Kuijpers MH, Kaufmann WS, Lammers JH, O'Callaghan JP, Pakkenberg B, *et al*. Regulatory

developmental neurotoxicity testing: a model study focussing on conventional neuropathology endpoints and other perspectives. Environ Toxicol Pharmacol. 2005;19: 745-55.
13. Breinan HA, Minas T, Hsu HP, Nehrer S, Sledge CB, Spector M. Effect of cultured autologous chondrocytes on repair of chondral defects in a canine model. J Bone Joint Surg Am. 1997;79:1439-51.
14. Lee CR, Grodzinsky AJ, Hsu HP, Spector M. Effects of a cultured autologous chondrocyte-seeded type II collagen scaffold on the healing of a chondral defect in a canine model. J Orthop Res. 2003;21:272-81.
15. Gundersen HJ, Jensen EB. The efficiency of systematic sampling in stereology and its prediction. J Microsc. 1987;147:229-63.
16. Boyce RW, Dorph-Petersen KA, Lyck L, Gundersen HJ. Design-based stereology: introduction to basic concepts and practical approaches for estimation of cell number. Toxicol Pathol. 2010;38:1011-25.
17. Tschanz SA, Burri PH, Weibel ER. A simple tool for stereological assessment of digital images: the STEPanizer. J Microsc. 2011;243:47-59.
18. Ross MH, Pawlina W. Cartilage (Chapter 7). In: *Histology*. Philadelphia, PA: Lippincott Williams & Wilkins; 2006:182.
19. Breinan HA, Hsu HP, Spector M. Chondral defects in animal models: effects of selected repair procedures in canines. Clin Orthop Relat Res. 2001(391 Suppl):S219-30.
20. Mouton PR. Principles and practices of unbiased stereology: an introduction for bioscientists. Baltimore, MD: Johns Hopkins University Press; 2002.
21. Gundersen HJ, Osterby R. Optimizing sampling efficiency of stereological studies in biology: or "do more less well!" J Microsc. 1981;121:65-73.
22. Cullen-McEwen LA, Armitage JA, Nyengaard JR, Moritz KM, Bertram JF. A design-based method for estimating glomerular number in the developing kidney. Am J Physiol Renal Physiol. 2011;300:F1448-53.
23. Chen F, Wegener G, Madsen TM, Nyengaard JR. Mitochondrial plasticity of the hippocampus in a genetic rat model of depression after antidepressant treatment. Synapse. 2013;67:127-34.
24. Kamp S, Balkert LS, Stenderup K, Rosada C, Pakkenberg B, Kemp K, *et al*. Stereological estimation of epidermal volumes and dermo-epidermal surface area in normal skin. Dermatology. 2011;223:131-9.
25. Ochs M, Muhlfeld C. Quantitative microscopy of the lung: a problem-based approach. Part 1: basic principles of lung stereology. Am J Physiol Lung Cell Mol Physiol. 2013;305: L15-22.
26. Østergaard KH, Baandrup UT, Wang T, Bertelsen MF, Andersen JB, Smerup M, *et al*. Left ventricular morphology of the giraffe heart examined by stereological methods. Anat Rec (Hoboken). 2013;296:611-21.
27. Luciw PA, Oslund KL, Yang XW, Adamson L, Ravindran R, Canfield DR, *et al*. Stereological analysis of bacterial load and lung lesions in nonhuman primates (rhesus macaques) experimentally infected with *Mycobacterium tuberculosis*. Am J Physiol Lung Cell Mol Physiol. 2011;301:L731-8.
28. Gundersen HJ, Boyce RW, Nyengaard JR, Odgaard A. The Conneulor: unbiased estimation of connectivity using physical disectors under projection. Bone. 1993;14: 217-22.
29. Foldager C, Bendtsen M, Zou X, Zou L, Olsen AK, Munk OL, *et al*. ISSLS prize winner: positron emission tomography and magnetic resonance imaging for monitoring interbody fusion with equine bone protein extract, recombinant human bone morphogenetic protein-2, and autograft. Spine (Phila Pa 1976). 2008;33:2683-90.
30. Baas J. Adjuvant therapies of bone graft around non-cemented experimental orthopedic implants stereological methods and experiments in dogs. Acta Orthop Suppl. 2008;79:1-43.
31. Vesterby A, Gundersen HJ, Melsen F, Mosekilde L. Marrow space star volume in the iliac crest decreases in osteoporotic patients after continuous treatment with fluoride, calcium, and vitamin D2 for five years. Bone. 1991;12:33-7.
32. Keller KK, Thomsen JS, Stengaard-Pedersen K, Dagnaes-Hansen F, Nyengaard JR, Hauge EM. Bone formation and resorption are both increased in experimental autoimmune arthritis. PLoS One. 2012;7:e53034.
33. Mathieu C, Chevrier A, Lascau-Coman V, Rivard GE, Hoemann CD. Stereological analysis of subchondral angiogenesis induced by chitosan and coagulation factors in microdrilled articular cartilage defects. Osteoarthritis Cartilage. 2013;21:849-59.
34. Långsjö TK, Vasara AI, Hyttinen MM, Lammi MJ, Kaukinen A, Helminen HJ, *et al*. Quantitative analysis of collagen network structure and fibril dimensions in cartilage repair with autologous chondrocyte transplantation. Cells Tissues Organs. 2010;192:351-60.
35. Lafantaisie-Favreau CH, Guzmán-Morales J, Sun J, Chen G, Harris A, Smith TD, *et al*. Subchondral pre-solidified chitosan/blood implants elicit reproducible early osteochondral wound-repair responses including neutrophil and stromal cell chemotaxis, bone resorption and repair, enhanced repair tissue integration and delayed matrix deposition. BMC Musculoskelet Disord. 2013;14:27.
36. Heir S, Aroen A, Loken S, Sulheim S, Engebretsen L, Reinholt FP. Intraarticular location predicts cartilage filling and subchondral bone changes in a chondral defect. Acta Orthop. 2010;81:619-27.
37. Kreuz PC, Steinwachs MR, Erggelet C, Krause SJ, Konrad G, Uhl M, *et al*. Results after microfracture of full-thickness chondral defects in different compartments in the knee. Osteoarthritis Cartilage. 2006;14:1119-25.
38. Kreuz PC, Erggelet C, Steinwachs MR, Krause SJ, Lahm A, Niemeyer P, *et al*. Is microfracture of chondral defects in the knee associated with different results in patients aged 40 years or younger? Arthroscopy. 2006;22:1180-6.
39. Minas T, Gomoll AH, Rosenberger R, Royce RO, Bryant T. Increased failure rate of autologous chondrocyte implantation after previous treatment with marrow stimulation techniques. Am J Sports Med. 2009;37:902-8.
40. Mechlenburg I, Nyengaard JR, Gelineck J, Soballe K. Cartilage thickness in the hip joint measured by MRI and stereology—a methodological study. Osteoarthritis Cartilage. 2007;15:366-71.

41. Mechlenburg I, Nyengaard JR, Gelineck J, Soballe K, Troelsen A. Cartilage thickness in the hip measured by MRI and stereology before and after periacetabular osteotomy. Clin Orthop Relat Res. 2010;468:1884-90.
42. Foldager CB, Bünger C, Nielsen AB, Ulrich-Vinther M, Munir S, Everland H, *et al*. Dermatan sulphate in methoxy polyethylene glycol-polylactide-co-glycolic acid scaffolds upregulates fibronectin gene expression but has no effect on in vivo osteochondral repair. Int Orthop. 2012;36: 1507-13.
43. Christensen BB, Foldager CB, Hansen OM, Kristiansen AA, Le DQ, Nielsen AD, *et al*. A novel nano-structured porous polycaprolactone scaffold improves hyaline cartilage repair in a rabbit model compared to a collagen type I/III scaffold: in vitro and in vivo studies. Knee Surg Sports Traumatol Arthrosc. 2012;20:1192-204.